Design Issues for Encodings for Inter-Satellite Optical Communications using Single Photon Avalanche Detectors

Thomas Schwarz
Department of Computer Science
Marquette University
Milwaukee, Wisconsin, USA
thomas.schwarz@marquette.edu, orcid: 0000-0003-4433-3360,

***Abstract*—Optical line-of-sight communication in deep space uses lasers for signal creation and Single-Photon Avalanche Diodes (SPAD) for reception. In the ideal case, a single photon or its absence is needed to send one bit. In reality, neither transmission nor reception are perfect. The natural approach uses On-Off encoding where a bit is represented by a burst or its absence. Decoding then uses a simple threshold. In the harsh environment of space, SPAD deteriorate and will develop significant dead-count, where a non-existing photon is captured. On the other hand, not every photon is detected. The error probabilities are not symmetric. We find here that belief propagation is the only way to prepare raw photon detection numbers for submission to an error and erasure correcting code.**

I. Introduction

Single-Photon Avalanche Diodes (SPAD) can detect single photons with a high probability and a time delay jitter of pico-seconds. These characteristics allow SPAD to serve as receptors for optical communication where laser bursts or their absences transmit single bits. The resulting communication channel has asymmetric error characteristics. A photon is only detected with high probability, but on rare occasions, a non-existing photon is registered by a SPAD. This is called a dark-count. Exposure to radiation, as is common in space, apparently leads to SPAD degradation that results in higher dark-count but does not degrade the single photon discovery rate [6], [13]. If we use on-off coding, where – let's say – a one-bit is represented by a laser burst, and if we assume that only a handful of photons is captured at the SPAD during a burst, then $1 \to 0$ errors occur at a higher rate than $0 \to 1$ errors.

We investigate the design issues for the error control coding for communication using lasers and SPADs in space. In-space, optical communication faces different challenges than terrestrial communication. As latencies are very high, frequent acknowledgments and retransmissions of packets with unresolved errors are not opportune. This places very high requirements on error control.

The design of a complete error control system is beyond the scope of this paper. Instead, we focus on sending symbols, single bits or small groups of bits such as a nibble (half-byte) and explore alternatives to simple on-off encoding. To supplement a less error- and erasure-prone transmission of symbols, we need an Error and Erasure Control Code, that further reduces the error rates to almost nil and corrects all erasures. This second-stage code can profit from the information originally contained in the capture records at the SPAD. Presumably, the most successful code for this purpose will be a Low Density Parity-Check (LDPC)-code using some type of belief propagation. The first stage which we treat here uses local information, whereas the second stage can combine symbols or bits taken at a distance from the sent message and thus use global information.

We make a number of assumptions. First, the rate at which photons arrive at the SPAD is very limited. Second, we assume that the parameters of the SPAD are measurable *in situ* and change only slowly over time. This allows us to calculate error probabilities and use belief propagation based on the SPAD characteristics such as dark-count rate and Single Photon Detection Efficiency (SPDE) for decoding. For aggressive burst timing, the probability of more than two dark-counts is exceedingly small, so that capture of three or more photons during a burst interval indicates a burst with vanishingly small probability of an error. We exploit this type of information. On the other hand, a capture of no or only one photon carries much less information about the sent message. We find that we can improve on the naive on-off encoding scheme. Manchester encoding has very small error rates for single bits, but generates a large proportion of erasures. Adding parity bits and using Maximum Likelihood (ML) decoding for small symbols shows both a small reduction in error rates (when compensating for the overhead) and more reasonable erasure rates.

In what follows, we first discuss SPAD and the consequences of their exposure in space. We then look at ways to employ On-Off coding, Manchester encoding, and two versions of ML coding, of which only one convinces.

II. Modeling SPAD

An Avalanche Photo-Diode (APD) is a solid-state device built from a four layer semi-conductor built around a p-n

979-8-3315-2096-0/25/$31.00 ©2025 IEEE

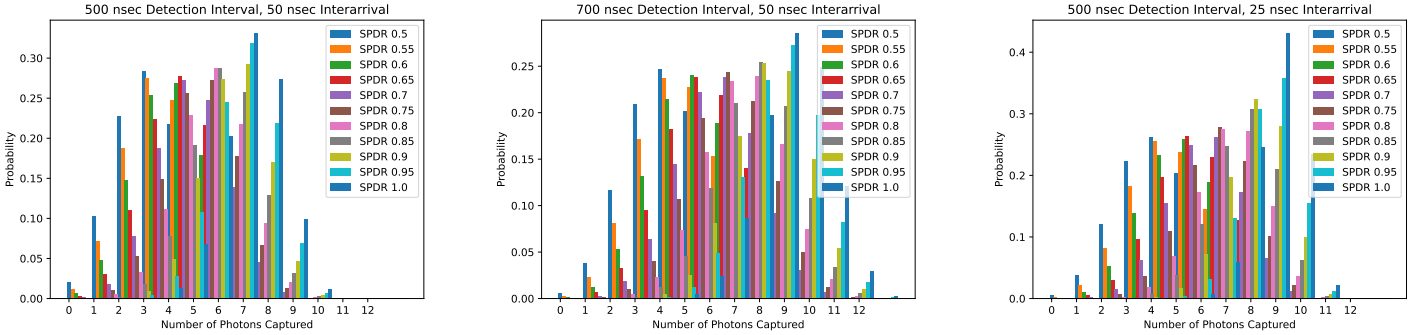

Fig. 1: Photon counts for various SPDE and Burst Length of 500 nsec and 700 nsec and a photon inter-arrival rate of 25 and 50 nsec.

junction. An APD uses the photoelectric effect, which converts light into electricity. The application of a high reverse voltage multiplies the charges generated by the impact of a photon through an electron avalanche effect. In *linear mode*, the applied voltage is less than the breakdown voltage of the p-n junction, and the number of carriers generated by the absorption of photons is more important the the ones generated by the avalanche effect. Thus, the number of generated carriers is proportional to the number of photons absorbed. In *Geiger* mode, the device is biased above the breakdown voltage of the p-n junction. A photon captured creates a high avalanche current. The multiplier effect far outweighs the absorption effect. As a result, the device is now a *Single Photon Avalanche Diode* (SPAD), which detects a single photon absorption, but needs additional electronics to stop the avalanche current from growing until it destroys the device [1], [2], [5], [7], [10].

The most prominent performance figure for SPAD is the *Single Photon Detection Efficiency* (SPDE) the ratio of detected photons over the number of photons striking the surface of the SPAD, also given as the *Single Photon Detection Probability* (SPDP). Through steady advancement of technology, this number can be better than 90% and very close to 100%.

After an avalanche has been triggered and quenched, the SPAD enters a *reset dead time* until the bias and charge is reestablished and a new photon can trigger another avalanche. This process needs additional circuitry. When the rising edge of the avalanche current is sensed, an output pulse is created and simultaneously, the avalanche current is quenched in order to prevent the avalanche current to accumulate and thereby damage the device [5]. From the user perspective, the *dead time* is the time following a photon capture where no additional photon can be captured. Its length is in the tens of nanoseconds.

An avalanche can also be triggered by happenstance. This results in a *dark count*. The phenomenon is measured in the *dark count rate* in Hertz, i.e. events per second. In *after-pulsing*, the device reports a faulty photon capture shortly after a true capture. Its probability is between 0.5 and 2% [3]. In practice, devices seem to show rather idiosyncratic after-pulsing [14]. If SPADs are arranged in an array, the avalanche current can cause internal (to a SPAD-array) or external (between SPAD arrays) *cross talk* [3], [8]. Cross-talk probabilities are idiosyncratic to the array(s) but seem to be less than 1% [3].

TABLE I: Performance Characteristics of a single SPAD

Single Photon Detection Efficiency	50% - 100%
Dark Count Rate	10Hz – 1KHz
Dead Time	50 nsec
Burst Length	250 nsec – 600 nsec
Photon Inter-arrival Rate	50 nsec - 150 nsec
After-Pulsing Rate	0%

Space is a notoriously harsh environment. Experiments with exposing SPAD to radiation [6], [13] have shown their suitability for space applications. Gamma radiation has little effect though exposure with high energy particles can result in a permanent increase in the dark count rate of up to 1Khz. The SPDE was not affected. To mitigate, one can use redundancy in the number of SPAD [12]. Whereas earth-bound SPAD nowadays have very low dark-count rates, we have to assume that this is not the case for SPAD in space.

III. Counting Codes

The simplest mode of sending messages is to use On-Off coding, where a burst corresponds to a one-bit and its absence to a zero-bit (or vice-versa). The bursts and their absences take a multiple of the *detection time interval*. For receiving, the number of photons detected by the SPAD is translated into bits again. The length of the detection time interval determines the ability to recover the message without error. As we have seen, for an in-space application, we cannot assume that SPAD have no dark-counts. A dark-count during the detection interval can lead to mistake a sent zero for a one. Similarly, while a laser burst consists of a plethora of photons, only few will be available for detection at the SPAD. Since we can use a cautious mode where we refuse to decide between a zero and a one bit, we will also have to deal with erased bits. We will have to encode the message with an Error and Erasure Control Code (EECC) to reliably deal with errors and erasures. Because laser beams diverge over very long distances, the majority of emitted photons will not reach the SPAD. If we

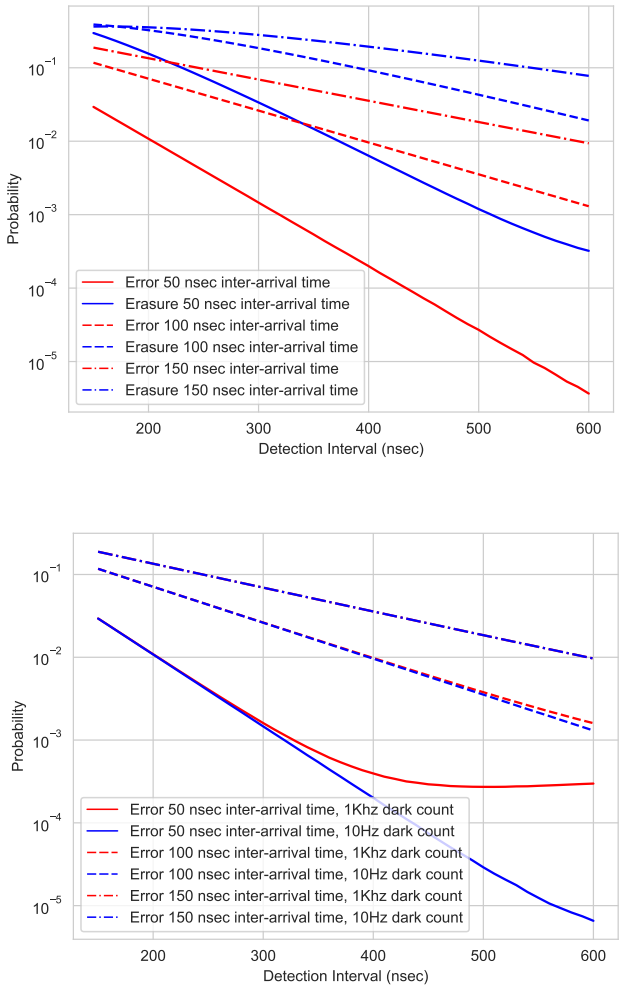

Fig. 2: Error and Erasure Probabilities for the cautious and the aggressive mode, 85% SPDP.

model this by applying a small probability that a photon out of a constant stream of photons reaches the SPAD, then the arrival of photons at the SPAD is governed by an exponential distribution with an average *inter-arrival time*.

We modeled the behavior of a SPAD with the parameters contained in Table I. We then assumed two different decoding modes for the simple method, the *cautious* one and the *aggressive* one. For the cautious method, we decide on a zero if no photon was detected, and on a one if two or more photons were detected. If one photon is detected, then we decide on an *erased* bit. We implemented a simulation (with 10^8 iterations) that obtains the number of photons discovered depending on whether in the previous detection interval a photon was detected or not. These numbers differ moderately because of the dead-time after a photon capture.

First, we look at the influence of the SPDP for long detection intervals, assuming a dark count rate of 1KHz. The results are given in Fig. 1. Even with this long detection times, there is a significant possibility of not registering a single photon during a burst.

Second, we evaluate our cautious encoding for an SPDP for 85%. It turns out that the dark-count rate has negligible effects. From Fig. 2 top, we can see that in order to have an expected erasure rate of less than 1%, we need a 50 nsec inter-arrival rate and a detection interval of 400 nsec. The capacity of the EECC needs to be more than that. At the minimum, the overhead of the EECC is the erasure probability plus at least two times the error probability. This means that on average 8 photons will need to hit the SPAD during a burst. Third, we calculated the probability that a bit is in error using the aggressive mode. There, the dark count rate is important. If the dark count rate is at 10Hz, we obtain an error rate of 10^{-3} for a detection interval of 330 nsec and an inter-arrival rate of photons at 50 nsec. This means on average 6.6 photons during a burst or 3.3 photons per bit, to which we have to add the overhead of the upper level error control code.

IV. Manchester Coding

Manchester coding is an attractive option to convert error rates into erasure rates. It divides the detection time interval into two equally sized parts. A 1 is sent as a burst in the first half followed by the absence of the burst and a 0 is sent as the absence of the burst in the first half and a burst in the second half. Of course, we can just as easily use the opposite convention. Manchester coding offers some additional benefits. First, there is always a "transition" – a switch fron a burst to a non-burst or vice versa – in the middle of the detection interval. This can be used to synchronize timing. Secondly, the longest burst is now caused by a 01 combination in the input and has the length of the detection interval. As cooling is difficult in vacuum, a more equitable use of the laser should make the engineering of the sender simpler.

To decode, we obtain the number of photons n_0 and n_1 in the first and second half of the detection interval. If $n_0 > n_1$, we decode as 1, if $n_0 < n_1$, we decode as 0, and if $n_0 = n_1$, we decode as an erasure.

To assess the performance of Manchester coding, we simulated SPAD performance for certain characteristics given in Tab. I. We made a distinction, as before, whether a burst was followed by a non-burst or not. From these simulation results, we can distill the probability of an erased bit and the probability of a bit in error. The latter is rather small since it means at least one dark count in the non-burst half-interval. The probability of erasure is always dominated by the probability that no photon of a burst is captured.

As we can see from Fig. 3, we are successful in moving the error rate to the erasure rate, even compared with the cautious mode. This is important, because it is much easier for a code to deal with erasures than to deal with errors. Unfortunately, Manchester encoding has not reduced the overall amount of error and erasure correction needed, but merely simplified the task. When Manchester encoding fails in an erasure, both bit values are equally likely, with the exception that a photon capture in the preceding detection interval makes a non-capture

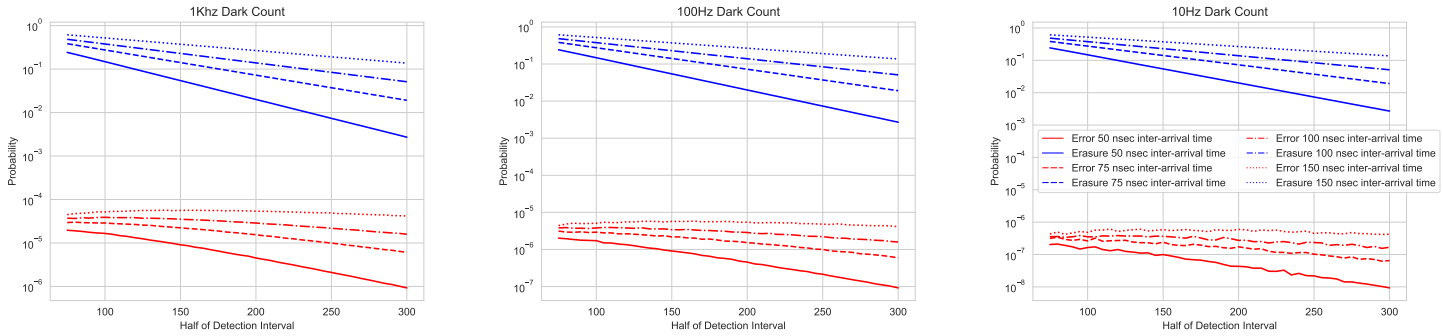

Fig. 3: Error and Erasure rates using Manchester Coding.

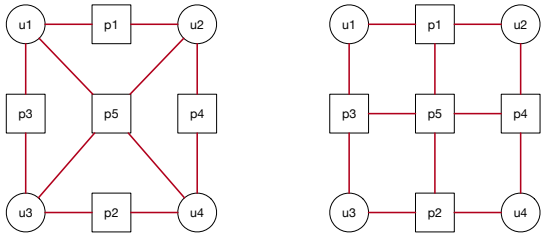

Fig. 4: Tanner Graph for our parity code. $p1 = 1 \oplus u_1 \oplus u_2$, $p2 = 1 \oplus u_3 \oplus u_4$, $p3 = 1 \oplus u_1 \oplus u_3$, $p4 = 1 \oplus u_2 \oplus u_4$, and $p5 = u_1 \oplus u_2 \oplus u_3 \oplus u_4$.

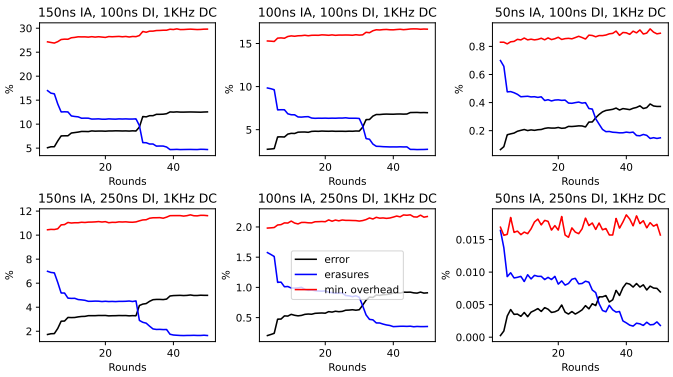

Fig. 5: Effectiveness of additional rounds during probability propagation depending on Inter-Arrival rates (IA), Detection Interval (DI), and a Dark Count (DC) of 1KHz. The SPDP is 85%.

during a following burst slightly more likely. Thus, if there is a capture in the preceding interval, then a 1-bit is more likely. However, quite a number of bits are not subject to an error (caused by the SPAD operation). If more than three photons are captured, then we can be sure of the sent value with almost complete certainty. Thus, Manchester encoding can pass on to the EECC-level some additional information.

V. Maximum Likelihood Encoding with Parities

The number of photons captured during a time interval follows a determined probability. Because of dead-time, this number depends partially on what was attempted to transmit in the previous time interval. Using Bayes' rule, we can then determine the probability that a one was sent given the amount of photons captured.

$$\text{Prob}\,(1 \text{ sent } | x \text{ capt.}) = \frac{\text{Prob}\,(x \text{ capt.} | 1 \text{ sent})\,\text{Prob}\,(1 \text{ sent})}{\text{Prob}\,(x \text{ capt.})}$$

We can safely assume that $\text{Prob}\,(1 \text{ sent}) = 1/2$. We obtained the other factors via simulation.

As we use these probabilities in the decoding, they need to be known during operations. What follows is therefore based on the capability to know at least approximately these probabilities. As SPAD degradation can be assumed to be slow, as estimates of dark count rates and SPDP can be maintained, and as software can be updated even in a satellite, we make this assumption in what follows.

We can use these probabilities in an EECC code. Again, we assume a two-stage encoding, with other words a product code, where the first stage uses small pieces of the message and the second stage is more global, where we concentrate here on the first stage. We break the original message into half-bytes (nibbles). We place the four bits into a 2×2 matrix, to which we add odd column and row parity as well as a global parity bit in order to obtain a 3×3 matrix. Thus, given a user message of (u_1, u_2, u_3, u_4), we actually send

$$\begin{pmatrix} u_1 & u_2 & 1 \oplus u_1 \oplus u_2 \\ u_3 & u_4 & 1 \oplus u_3 \oplus u_4 \\ 1 \oplus u_1 \oplus u_3 & 1 \oplus u_2 \oplus u_4 & u_1 \oplus u_2 \oplus u_3 \oplus u_4 \end{pmatrix},$$

row by row. We chose odd parity in order to prevent long bursts of zeroes. As a motivating example for the use of parity in decoding, we assume that we have captured $(0,1,2)$ photons. The most likely sent message is $(0,1,1)$ based on photon count, but this message is impossible, as it has even parity. We can use maximum-likelihood encoding, where we calculate the probability of any of the four legitimate messages $(0,0,1)$, $(0,1,0)$, $(1,0,0)$ $(1,1,1)$ given this particular pattern of captured photons. We can use this procedure for our scheme in using local and using global information.

We describe the local version first. The probabilities that a specific bit out of the nine transmitted is a 1 are linked

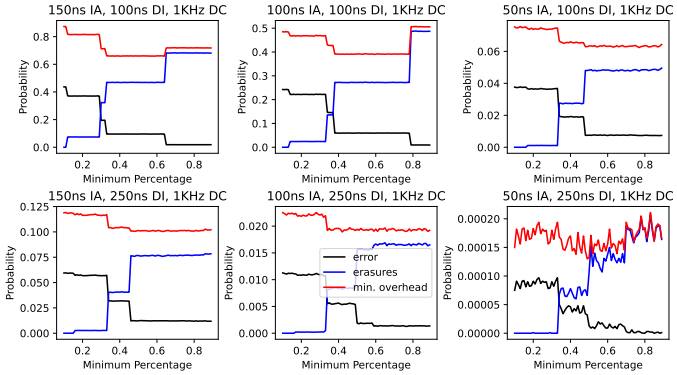

Fig. 6: Effectiveness of requiring minimum probability for the Maximum Likelihood Decoding depending on Inter-Arrival rates (IA), Detection Interval (DI), and a Dark Count (DC) of 1KHz. The SPDP is 85%.

through the parity equations, making this into a Markov Logic Network [9], [11]. The local version updates these probabilities by using the parity equations. As Tanner graph in Fig. 4 of our parity code has many graph cycles, so that the more efficient mechanism for belief propagation do not apply. (Because we use odd parities, the Figure does not give the classical Tanner graph, but a slight adaptation. Also, p_5 is $p_1 \oplus p_2$, which happens to be equal to $p_3 \oplus p_4$, which is not adequately presented in the graph.) Our ad hoc approach starts out by using the number of photons and Bayes formula in order to assign a probability to each bit. We then take a row and uses maximum likelihood encoding, which is simple as there are only four possible user messages namely $(0,0,1)$, $(0,1,0)$, $(1,0,0)$, and $(1,1,0)$. We continue for all rows and then continue with the columns using the newly updated probabilities. This constitutes a single round. We continue for several rounds. If eventually the probabilities converge to values very close to one or zero, then we can decode, otherwise we have an erasure. We prefer to call this method *Probability Propagation* (PP), as it is a form of belief propagation [4], but not a standard algorithm.

Using PP, we can use several numbers of rounds, where each round updates the probability of seeing this coefficient in the message using all rows and all columns. When we plot the resulting error and erasure probabilities (in percent) in Fig. 5, we see how error starts out very low, but increases, usually in two different steps, while the erasures behave in an opposite manner. Erasures are of course much more simple to deal with than erasures. Since in order to correct a single bit in error, we need at least two parity bits, whereas an erased bit only needs a single parity bit, we can estimate the complexity of the second stage code by multiplying the error rate with two and adding the erasure rate. This procedure always slightly underestimates the need. We need however at least two rounds. From results like the ones in Fig. 5, we estimate that using somewhere between five and ten rounds gives the optimal trade-off between error rate and erasure rate. We notice the curious step-wise behavior of the two rates over a large range of parameters.

An advantage of PP is its relatively benign asymptotic behavior as the number of rows and columns in a matrix grows as $O(\sqrt{n})$ in the number of bits in a symbol.

The second possibility uses Maximum Likelihood (ML) Decoding. Given a count of photons, we calculate the probability of all valid send messages and select the one with the highest probability. Sometimes, there is no single one. For example, if we capture nine times in a row no photon, then any one of the following matrices is equally likely

$$\begin{pmatrix} 0 & 0 & 1 \\ 0 & 0 & 1 \\ 1 & 1 & 0 \end{pmatrix}, \begin{pmatrix} 0 & 0 & 1 \\ 0 & 1 & 0 \\ 1 & 0 & 0 \end{pmatrix}, \begin{pmatrix} 0 & 1 & 0 \\ 1 & 0 & 0 \\ 0 & 0 & 1 \end{pmatrix}, \begin{pmatrix} 1 & 0 & 0 \\ 0 & 1 & 0 \\ 0 & 0 & 1 \end{pmatrix}.$$

In a case like this, decoding is likely to result in error. In general, picking the most likely sent message even if its overall probability is low will also likely result in an error. Similarly to our investigation of PP, we tried out various cutoff points to report the successful decoding of the capture result. We give some in Fig. 6. Based on the cumulative evidence, we require that the probability of the most likely sent message be at least 50%.

Extending ML to larger symbol sizes is of course possible, but as we increase the symbol size, the number of possibly sent messages increases exponentially. Finally, we use the sum-product message passing [9], which uses parity information on rows and columns simultaneously.

We compare PP, Maximum Likelihood (ML) decoding and Belief Propagation (BP) based on sum-product message passing in Fig. 7, 8, and 9. Clearly, PP and to a much lesser extent BP is dominated by ML. When we compare ML with Manchester encoding, we need to take cognizance of the different encoding overhead, which is 100% for Manchester Encoding and 120% for PP and ML. If we compare ML with Manchester encoding, we have a more complicated picture as the error rate of Manchester encoding is slightly lower, while the erasure rate is much higher. If we want to keep the error rate below 10^{-3}, we can choose a detection time of 140 nsec and an inter-arrival time of 50 nsec. Given the 125% parity overhead, this amounts to 6.3 photons per bit transmitted.

VI. Conclusion and Further Work

We started the investigation for line-of-sight communication using lasers and SPADs. We concentrated on the selection of small symbols (bits or nibbles) and their encoding. We found that Manchester encoding can push error rates towards erasure rates, the PP is not effective, whereas maximum likelihood decoding brings a slight improvement on the aggressive mode of naive decoding.

Even our investigation of encoding symbols (bits or several bits) is not complete. We did not report on the use of constant weight codes, as our results were not convincing.

The upper layer of EECC can use any one of the many codes developed over the last seven decades. These codes are often designed for symmetric errors, where bit flips are equally likely for both directions. With the exception of those using

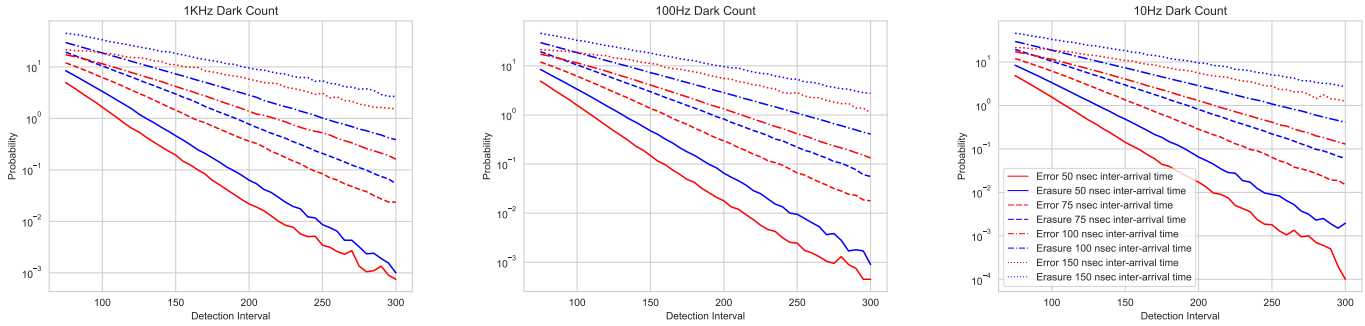

Fig. 7: Error and Erasure Rates for PP on a nibble at 85% SPDP.

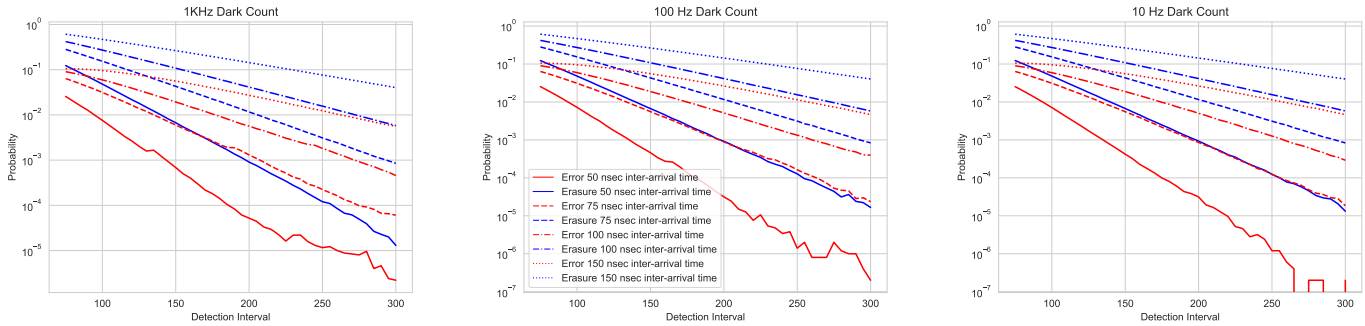

Fig. 8: Error and Erasure Rates for ML on a nibble at 85% SPDP.

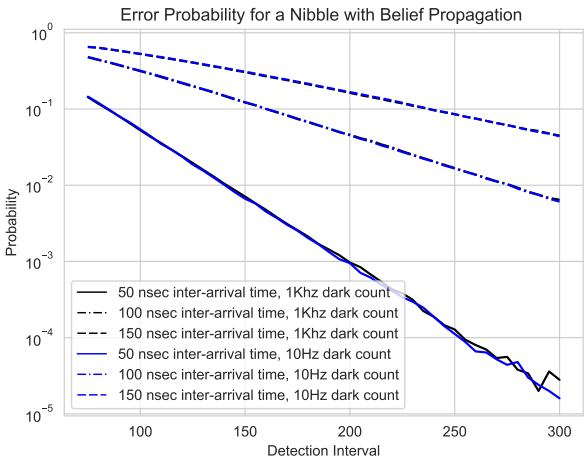

Fig. 9: Error rate for the Sum-Product form of belief propagation.

belief propagation techniques, they are usually not equipped to deal with the information that the lower EECC layer can provide. To wit, if we capture three or more photons during a detection interval, then we can conclude with overwhelmingly small probability of an error that we have detected a burst. However, if no photons were captured during a detection interval, then it is more likely that there was a non-burst than a burst, but the conclusion can only be made with an error probability of between 1% to 15%, depending on the length of the detection interval and the inter-arrival rate. The next step in our investigation will be directed towards exploiting this additional information.

REFERENCES

[1] F. Ceccarelli, G. Acconcia, A. Gulinatti, M. Ghioni, I. Rech, and R. Osellame, "Recent advances and future perspectives of single-photon avalanche diodes for quantum photonics applications," *Advanced Quantum Technologies*, vol. 4, no. 2, 2021. [Online]. Available: https://onlinelibrary.wiley.com/doi/abs/10.1002/qute.202000102

[2] A. Govdeli, J. N. Straguzzi, Z. Yong, Y. Lin, X. Luo, H. Chua, G.-Q. Lo, W. D. Sacher, and J. K. Poon, "Room-temperature waveguide-coupled silicon single-photon avalanche diodes," *NPJ Nanophotonics*, vol. 1, no. 1, p. 2, 2024.

[3] S. Jahromi and J. Kostamovaara, "Timing and probability of crosstalk in a dense CMOS SPAD array in pulsed TOF applications," *Optics express*, vol. 26, no. 16, pp. 20 622–20 632, 2018.

[4] D. K. Kythe and P. K. Kythe, *Algebraic and stochastic coding theory*. CRC Press Boca Raton (FL), 2012.

[5] C. Liu, H.-F. Ye, and Y.-L. Shi, "Advances in near-infrared avalanche diode single-photon detectors," *Chip*, vol. 1, no. 1, 2022.

[6] F. Moscatelli, M. Marisaldi, P. Maccagnani, C. Labanti, F. Fuschino, M. Prest, A. Berra, D. Bolognini, M. Ghioni, I. Rech, A. Gulinatti, A. Giudice, G. Simmerle, A. Candelori, S. Mattiazzo, X. Sun, J. F. Cavanaugh, and D. Rubini, "Radiation tests of single photon avalanche diode for space applications," *Nuclear Instruments and Methods in Physics Research Section A: Accelerators, Spectrometers, Detectors and Associated Equipment*, vol. 711, pp. 65–72, 2013. [Online]. Available: https://www.sciencedirect.com/science/article/pii/S0168900213001484

[7] L. Neri, S. Tudisco, L. Lanzanò, F. Musumeci, S. Privitera, A. Scordino, G. Condorelli, G. Fallica, M. Mazzillo, D. Sanfilippo, and G. Valvo, "Design and characterization of single photon avalanche diodes arrays,"

Nuclear Instruments and Methods in Physics Research Section A: Accelerators, Spectrometers, Detectors and Associated Equipment, vol. 617, no. 1, pp. 432–433, 2010, 11th Pisa Meeting on Advanced Detectors.

[8] B. Novakovic, K. Raymond, G. Gallina, L. Xie, F. Retiere, and D. McGuire, "Electro-optical simulation and characterization of DCR and secondary emission in SPADs," in *2022 International Conference on Numerical Simulation of Optoelectronic Devices (NUSOD)*. IEEE, 2022, pp. 3–4.

[9] J. Pearl, *Probabilistic reasoning in intelligent systems: networks of plausible inference*. Elsevier, 2014.

[10] X. Qian, W. Jiang, A. Elsharabasy, and M. J. Deen, "Modeling for single-photon avalanche diodes: State-of-the-art and research challenges," *Sensors*, vol. 23, no. 7, 2023. [Online]. Available: https://www.mdpi.com/1424-8220/23/7/3412

[11] M. Richardson and P. Domingos, "Markov logic networks," *Machine learning*, vol. 62, pp. 107–136, 2006.

[12] J. A. Smith, G. Acconcia, I. Rech, R. J. Hare, and C. A. Hostetler, "Terahertz photon counting: large-format SPAD arrays for lidar remote sensing of the atmosphere and ocean from space," in *Advanced Photon Counting Techniques XIV*, vol. 11386. SPIE, 2020, pp. 17–27.

[13] M.-L. Wu, F. Gramuglia, E. Ripiccini, C. A. Fenoglio, E. Kizilkan, P. Keshavarzian, K. Morimoto, L. Paolozzi, C. Bruschini, and E. Charbon, "CMOS SPADs for high radiation environments," in *Proceedings, IEEE Nuclear Science Symposium and Medical Imaging Conference (NSS/MIC)*, 2022.

[14] A. W. Ziarkash, S. K. Joshi, M. Stipčević, and R. Ursin, "Comparative study of afterpulsing behavior and models in single photon counting avalanche photo diode detectors," *Scientific reports*, vol. 8, no. 1, pp. 1–8, 2018.